*DISTRIBUTION STATEMENT A. Approved for public release; distribution is unlimited.*

# APL - North Pacific Acoustic Laboratory

PI James A. Mercer
Applied Physics Laboratory, University of Washington
1013 NE 40th Street
Seattle, WA 98105
phone: (206) 543-1361 fax: (206) 543-6785 email: mercer@apl.washington.edu

CO-PI Rex Andrew
on grant N00014-08-1-0843
Applied Physics Laboratory, University of Washington
1013 NE 40th Street
Seattle, WA 98105
phone: (206) 543-1250 fax: (206) 543-6785 email: rex@apl.washington.edu

CO-PI Andrew White
on grant N00014-08-1-0200
Applied Physics Laboratory, University of Washington
1013 NE 40th Street
Seattle, WA 98105
phone: (206) 685-3529 fax: (206) 543-6785 email: andrew8@apl.washington.edu

http://www.apl.washington.edu/projects/blue_water/index.html

## LONG-TERM GOALS

The ultimate limitations to the performance of long-range sonar are due to ocean sound speed perturbations and the characteristics of the ambient acoustic noise field. Scattering and diffraction resulting from internal waves and other ocean processes limit the temporal and spatial coherence of the received signal, while the ambient noise field is in direct competition with the received signal. Research conducted in the North Pacific Acoustic Laboratory (NPAL) program at the Applied Physics Laboratory (APL-UW) is directed toward a complete understanding of the basic physics of low-frequency, long-range, deep water, broadband acoustic propagation, the effects of ocean variability on signal coherence, and the fundamental limits to signal processing at long-range that are imposed by ocean processes. The long-term goal of NPAL is to optimize advanced signal processing techniques, including matched-field processing and adaptive array processing methods, based upon knowledge about the multi-dimensional character of the propagation and noise fields and their impact on long-range ocean acoustic signal transmissions.

## OBJECTIVES

The scientific objectives of the North Pacific Acoustic Laboratory are:

1. To study the spatial and temporal coherence of long-range, low-frequency resolved rays and modes and the dependence upon ocean processes, transmission distance, and signal frequency.
2. To explore the range and frequency dependence of the higher order statistics of resolved ray and mode arrivals and of the highly scattered finale observed in previous experiments.
3. To define the characteristics and trends, and determine the relative causes of low-frequency ambient noise on ocean basin scales.
4. To elucidate the roles of internal waves, ocean spice, internal tides, fronts and eddies in causing fluctuations in acoustic receptions.
5. To improve basin-scale ocean sound-speed predictions via assimilation of acoustic travel-time and other data into numerical ocean-dynamic models.
6. To fully analyze our experiment in the Philippine Sea, the results of which will support all of the objectives listed above.

## APPROACH

APL-UW employs a combination of experimental measurements, data analysis, simulations, and theoretical development to address the objectives outlined above. These activities are funneled through two primary avenues. ***The North Pacific Ambient Noise Laboratory***, operated and maintained by APL-UW, provides a full-time laboratory for real-time acoustic measurements at a selection of basin-scale locations, the capability to test various transmission signals, and ambient noise (including marine mammals) measurements in the NE Pacific Ocean. The Laboratory consists of the legacy SOSUS hydrophone receiver network in the Pacific Ocean, and a data processing and archive center at the Applied Physics Laboratory. Hydrophone arrays designated as D, E, F, and R have been declassified. Arrays we designate as G, H, I, J, K, L, M, N, O, P, and T remain classified.

The second avenue includes highly focused, comparatively short-term experiments.
We have completed a pilot study/engineering test and an experiment in the ***Philippine Sea*** called **PhilSea9** and **PhilSea10**, respectively [1]. See Figure 1. The principal elements of the APL-UW effort during the 2010 experiment were: 1) a 55-hour continuous transmission from ship stop SS500 at 500 km from the DVLA and a depth of 1000 m, 2) a tow of a CTD Chain along the path toward the Distributed Vertical Line Array (DVLA) from SS500, 3) a source tow at a depth of 150 m at ranges between 25 and 43 km from the DVLA through the region of a Reliable Acoustic Path (RAP) from the near-surface region to the water column bottom, 4) a series of CTD casts every 10 km from the DVLA back to SS500, and 5) a 55-hour continuous transmission from SS500 at a depth of 1000 m to the DVLA. The primary institutions participating in PhilSea10 were APL-UW, the Scripps Institution of Oceanography (SIO), and the Massachusetts Institute of Technology (MIT). Analysis of environmental data from PhilSea10 is underway, and we have now received the acoustic data from the DVLA.

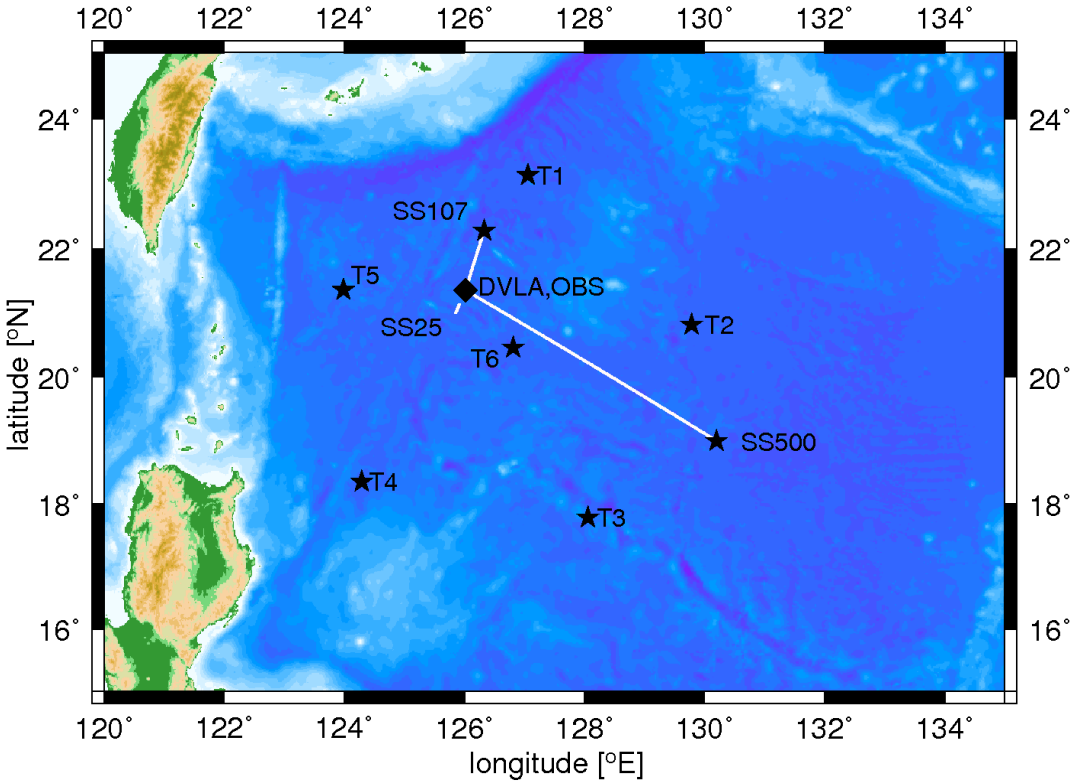


***Figure 1. Principal activity locations for PhilSea9 and PhilSea10***

## WORK COMPLETED

Although our current effort is focused on the avenues described above, a large number of publications are also still coming from previous experimental work, e.g., LOAPEX [2] (See the Publications section.).

### *North Pacific Ambient Noise Laboratory-*

The NPAL North Pacific Ambient Noise Laboratory was installed in the early 1990s as part of the Acoustic Thermometry of Ocean Climate program and utilizes undersea hydrophone arrays owned by the US Navy. In addition, shore-based equipment is located at Navy and non-Navy shore facilities. Complicating the transfer of data media and hardware components from the shore sites to APL-UW are the required auditable trails of information on storage media and hardware. The current procedures, protocols, and documentation requirements devised and negotiated by APL-UW and Navy personnel for these transfers are described in Ref [3].

Like most older electronic hardware, maintenance is a continuing issue. Hindering our monitoring and maintenance efforts for arrays J, K, L, M, N, O, P and T has been a loss of our secure communication link to the shore facility. The problem began with the requirement for a new type of secure transfer

hardware. After much frustration with the new hardware it was finally determined that the hardware was defective. Now that the hardware has been replaced it appears to be incompatible with the University of Washington's modem exchange system. Recent successes from an off-site location using XFINITY via Comcast have been successful. This commercial system may be the solution going forward.

Other significant problems for these sites include 1) hung computers (obviously this can be addressed more effectively once a remote communication link is established; 2) system hard drives that become full without the monitoring capability ( Site visits to service these receivers have recovered nearly 200GB of data. These data have been transferred manually to the APL Data Center for archiving.); 3) Empty data files due to IRIG timing channel dropouts (A software upgrade has solved the loss of data but the cause of the IRIG channel glitch is still unknown.); and 4) Motherboard failures (The problem is related to cooling fan failures. Unfortunately, these motherboards are no longer manufactured. Replacement boards are being identified.).

The shore station for receiver site R has been located at Naval Air Station, Barbers Point, HI. Due to several failures of the air conditioning (A/C) system, a remotely monitored temperature indicator was installed. A subsequent failure of the A/C system was detected and system down time was significantly reduced.

Following the Base Realignment and Closure action for NAS Barbers Point, the Site R building remained available as a shore site for several years until recently. All APL-UW equipment for site R was re-calibrated, removed and placed in storage in Hawaii. A portion of the cable route for site R will remain on Navy controlled property. Application to a land-board has been submitted to re-locate the receiver equipment over the cable route on this Navy controlled property. Since it is apparently more difficult to get approval for a temporary facility, a new facility of some type will be required.

Receiver arrays E and F terminate at a building on San Nicholas Island, CA. This facility has been closed and is no longer available. The APL-UW equipment will have to be removed. We are waiting for Navy approved transportation to San Nicholas Island to accomplish this task.
Routine remote checks from Seattle of the transmitter site on Kauai indicate that the system is still fully functional.

The distribution of one-hour ambient noise level data over a single year at all of our North Pacific receiver sites became of interest to the NOAA Sound Mapping group. In this case, the level measure is the arithmetic average over one hour. Statistics for arrays D, F, G and H have previously been published in the open literature, but extracting the statistics for these one-hour averages was a simple matter of adjusting some post-processing code and applying it to the calibrated archival datasets for those sites.

The procedure was not as simple for arrays J, K, L, M, N, O, P, and T. Fully calibrated archival data have never been produced for these sites --- the missing correction factor involves the transfer function of an interface card in the APL instrumentation rack, which introduced 1 to 3 dB of frequency dependent loss. Correction files were built for all these sites. Once this was done, the archival data (collected up to approximately 2007) was further processed to produce data calibrated with all known correction functions, and then compiled into one-hour level statistics for a given year. The results for sites D, F, G, H, J, K, L, M, N, O, P, and T were written to portable binary netCDF files and sent to HLS Research, La Jolla, California. Results for site K are shown in Figure 2.

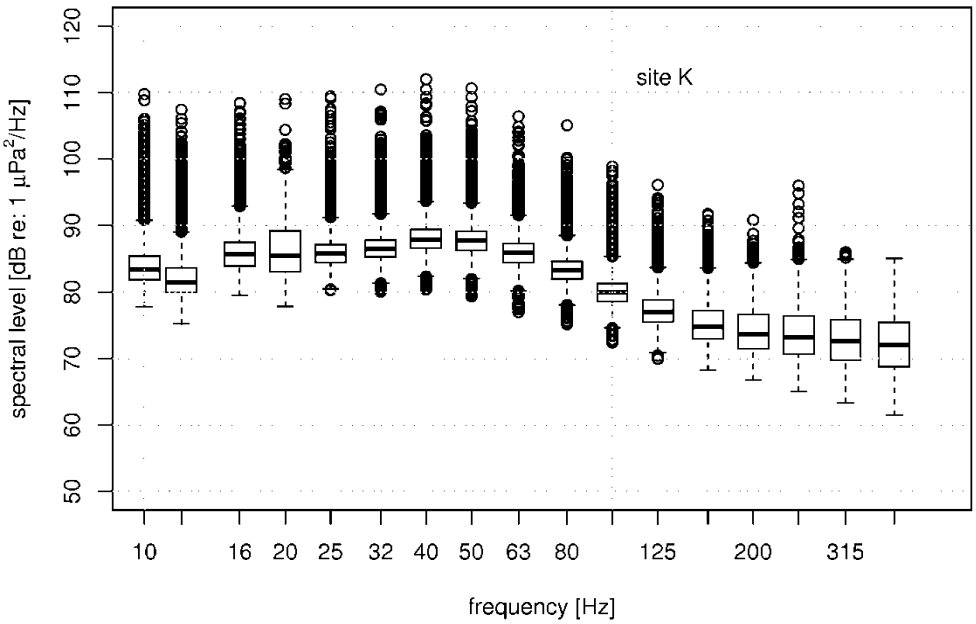


***Figure 2. One-hour average ambient noise level for site K.***

## NEW RESULTS

### *Philippine Sea-*

The detection and removal of outliers from the **Philsea09** acoustic dataset has allowed progress in analysis. Sources of contamination of the data included noise due to passing ships, glitches in the power amplifier that supplied the signal to the projector, and unidentifiable man-made signals in the water. The affected data were marked and removed. The result of this cleanup effort may be seen by comparing the bottom panel of Figure 4 of this report with the top panel of Figure 3 from the FY2011 annual report.

Time-independent and time-dependent Monte Carlo PE modeling efforts were described in the FY2011 annual report. These simulations required generation of random instances of displacement fields described by the GM81 model spectrum. Following Colosi and Brown [4] these displacements were converted to perturbed sound-speed fields using an approximation originally suggested by Stan Flatte [5]. The approximation is that the $N^2$ profile may be used in lieu of the potential sound speed gradient for perturbation of the background sound speed profile by the internal wave displacements. This approximation seems to have been applied, for example, by Xu [6] in MCPE (Monte Carlo Parabolic Equation) modeling. The validity and effect of the approximation in the Philippine Sea were not known, and therefore we conducted a comparison between this approximation and the more accurate model, which instead uses the potential sound speed gradient to calculate the perturbed sound-speed field.

The comparison involved writing a C-language code to compute the perturbed sound-speed field with the second, more accurate method and performing a time-independent MCPE experiment that employed this new code. Approximately 225 random perturbed sound-speed fields were used in the model experiment. The MCPE predictions for the scintillation index (SI) using the $N^2$ approximation vs. the potential sound speed gradient are shown in Figure 3, along with estimates of the SI made from the **Philsea09** acoustic data. This work was presented at the ASA Hong Kong conference.

The MCPE modeling efforts described above (and more completely in the FY2011 report) might be thought of as a possible pre-experiment scenario. As mentioned previously, these models included as a background environment low-passed, averaged sound-speed and $N^2$ profiles that were made using CTD casts taken during the 2009 cruises. We could have used, alternatively, profiles of the same quantities from the Levitus database. Aside from this detail, before conducting the **Philsea09** and **Philsea10** experiments, we had no more information about sources of fluctuation of the sound-speed field in the region, and in particular, about appropriate values for the parameters of the GM spectrum. Aside from the CTD profiles collected during the experiment, the ocean models used in these modeling efforts were not adjusted according to, for example, the environmental measurements made by the CTD sensors on the DVLA. An interesting question might be, "How well can we do at predicting acoustic intensity fluctuation measures using MCPE with a GM spectrum, without spending the time and money to measure the local fluctuations in sound speed?"

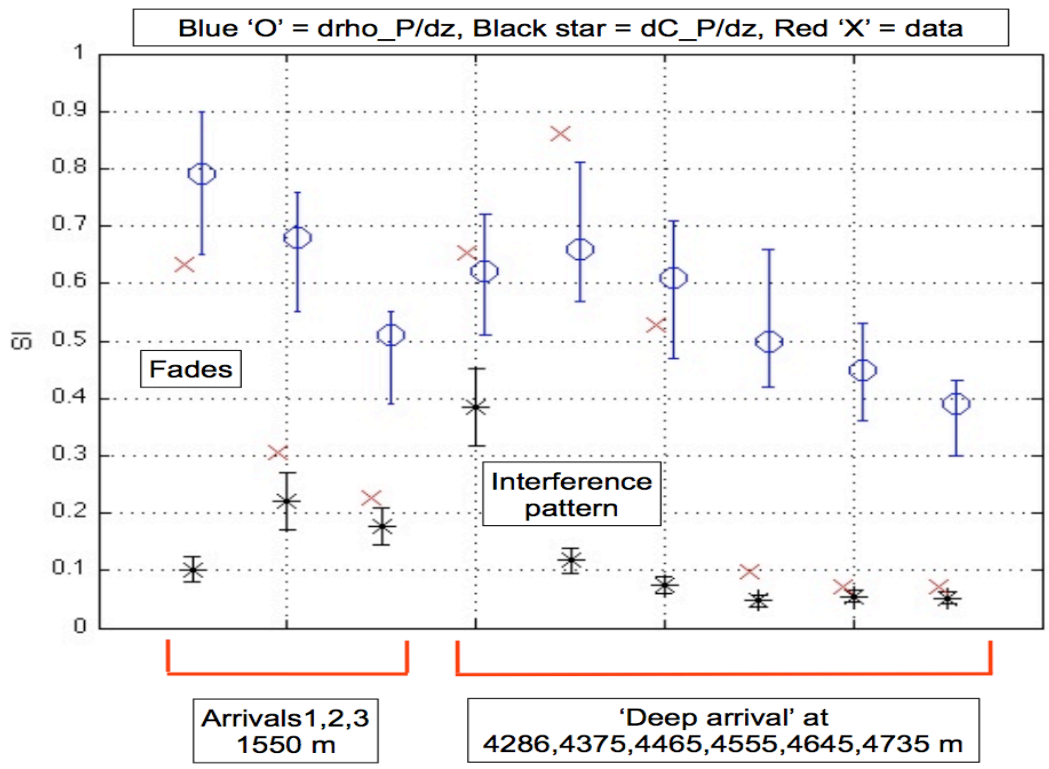


***Figure 3. Shown here are the MCPE model predictions of SI using the N^2 approximation (blue circle) vs. using the potential sound speed derivative (black star) in calculating the perturbed sound speed field from the displacement. The SI estimates made from philsea09 measurements (red x) are shown for comparison. The boxes labeled "Fades" and "Interference pattern" are discussed in the section describing the mixed-layer hypothesis.***

The above question is posed making at least one significant assumption: that the GM spectrum is an accurate representation of sound-speed fluctuations in the Philippine Sea. It is apparent from the APL/UW **Philsea10** 500 km CTD transect that there is a strong large-scale range-dependence to the sound speed profile. In addition, peaks at tidal frequencies are observed in the spectrum of sound speed variability measured by the CTD sensors on the DVLA. These two pieces of evidence suggest that a range-independent background sound-speed field perturbed by GM spectrum internal waves would not be a complete model of the Philippine Sea propagation environment. Construction of a model or models that address these concerns has been proposed for future work. This proposed work would go beyond the standard MCPE approach, however, which has generally made the same assumptions outlined above [6,7]. We are planning to adjust the "strength parameter" in the MCPE model as a part of our future work; this result may be later compared with more involved models that we have proposed to investigate. The adjusted-strength models may also be compared to our previous modeling as a simple first-cut attempt at answering the question posed in the previous paragraph.

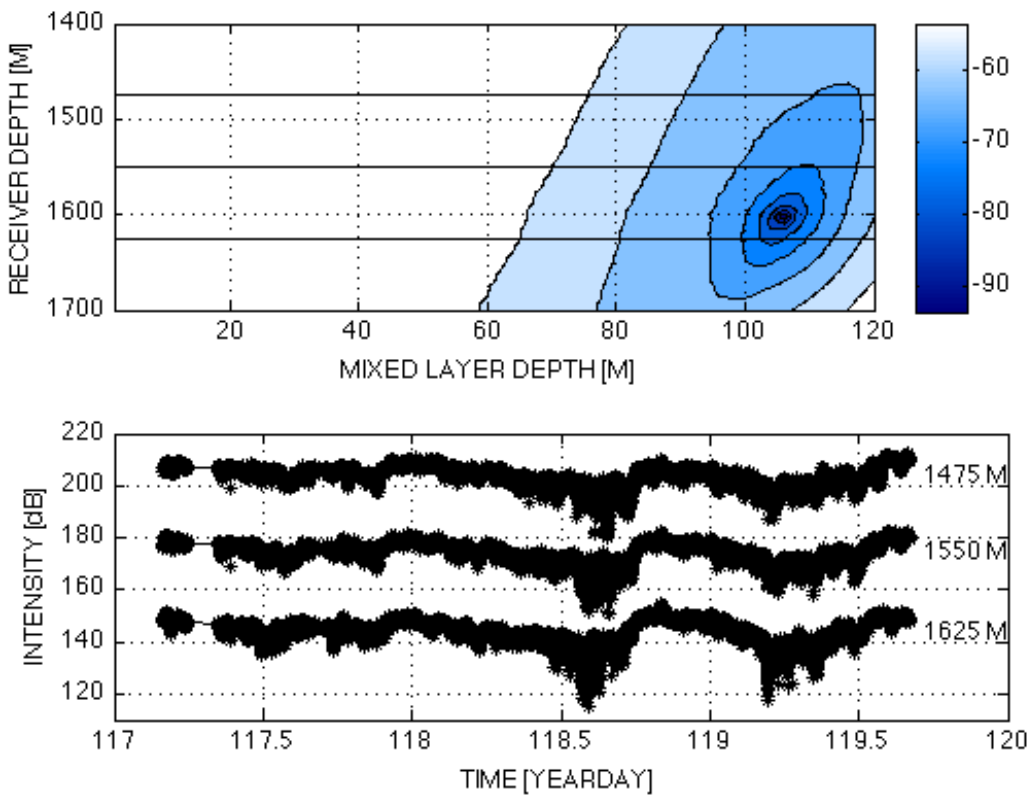


***Figure 4. The upper panel shows the predicted acoustic intensity for the shallow-turning path for receiver depths from 1400 to 1700 m vs mixed layer depth. Five dB contours of intensity are plotted. The horizontal black lines represent the depths of the hydrophones referred to in the lower panel. The lower panel shows the observed acoustic intensity for hydrophones at 1475, 1550, and 1625 m depth, as indicated by labels to the right of each record. An offset has been added to each timeseries for visualization.***

We have now also analyzed the CTD data collected on the DVLA in order to make an estimate of the GM strength parameter. Significant (up to 90 m) blow-downs of the DVLA occurred during the month of its deployment. These blow-downs introduced fluctuations into the temperature and salinity records relating to the change of depth of the sensors. The measurements were interpolated in depth in order to attempt to remove this instrument-caused fluctuation. Several interpolation methods were examined. The estimate of GM strength was much more strongly influenced by the choice of filter used to eliminate frequencies outside the internal wave spectral bounds than by the choice of interpolation method. An estimate of the GM strength appropriate for the Philippine Sea was made and the MCPE model adjusted accordingly. These simulations are currently running, and the results will be presented at a later date.

During the 2009 pilot study **PhilSea09**, deep (roughly ten dB) fades in acoustic intensity lasting for several hours were observed on hydrophones at several depths spanned by the shallow array. These fades were observed in acoustic arrivals having shallow upper turning points (~60 m), and not in arrivals with deeper upper turning points (~200 m). The observed fades were not predicted by time-dependent Monte Carlo Parabolic Equation (MCPE) modeling with random GM internal wave displacements of a range-independent background.

Some of the mismatch between Monte Carlo PE and the observed intensity fluctuations is thought to be due to interaction with the mixed layer in **PhilSea09**. To explore this possibility, the same range-independent profile used in the MCPE modeling was modified to include a mixed layer. Results from acoustic mode propagation through the modified sound speed profile support this hypothesis; see Figures 4 and 5 of this report.

The 60-hour timeseries of acoustic intensity resulting from APL-UW transmissions in **PhilSea09** are shown in the bottom panel of Figure 4. Deep fades of similar magnitude are visible in the records at each of the three hydrophones, with an apparently high coherence. The top panel in Figure 4 shows the modeled effect of a mixed layer on the acoustic intensity for receiver depths including those of the hydrophones that recorded the deep fades. The mode-propagation modeling predicts fades of similar magnitude given the observed mixed layer depths, and also predicts a high coherence between the three receivers.

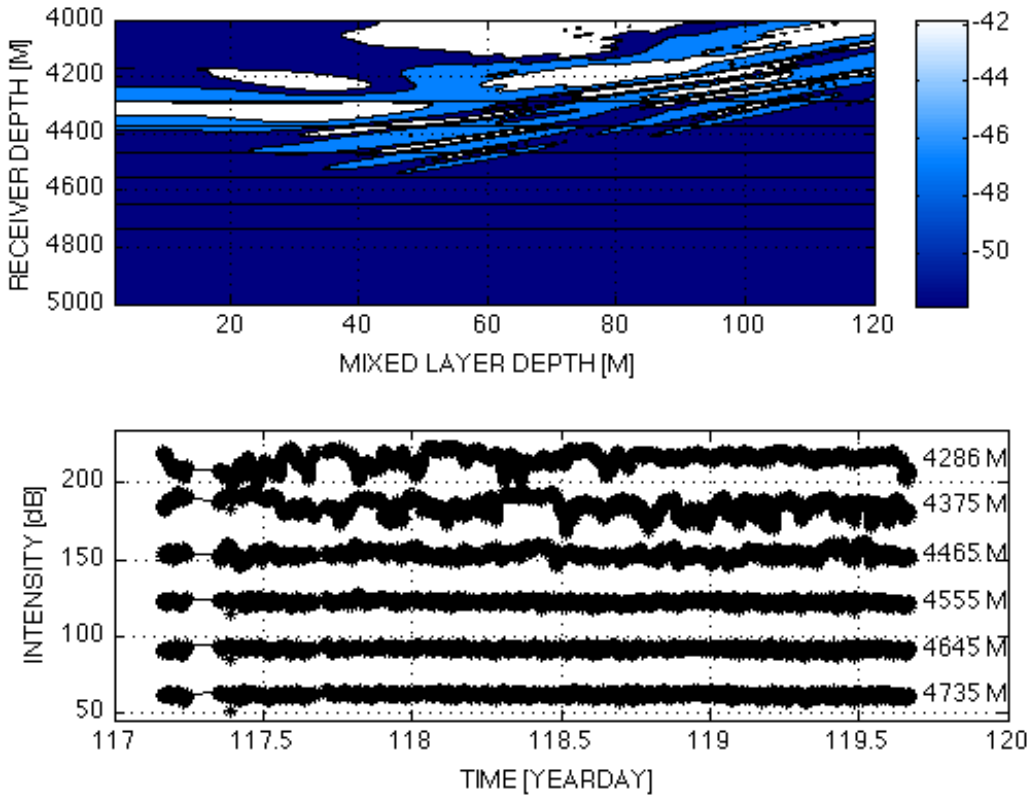


***Figure 5. The upper panel shows predicted acoustic intensity for a shallow-turning path forming the deep arrival for receiver depths between 4000 to 5000 m vs mixed layer depth. Five dB contours are plotted. The lower panel shows the observed acoustic intensity for six hydrophones on the deep array. An offset has been added to each timeseries for visualization.***

The bottom panel of Figure 5 shows the intensity timeseries from the same transmissions, recorded on the deep subsection of hydrophones on the DVLA. The intensity recorded at 4286, 4375, and 4465 m depth exhibits much larger fluctuations than the intensity recorded at depths of 4555, 4645, and 4735 m, and the intensity at the shallower three depths does not appear to be coherent.

The top panel of Figure 4 shows the modeled effect of a mixed layer. When the mixed layer is absent, or very shallow, the intensity varies for the top three receivers by up to ten dB. As the mixed layer deepens, a complicated interference pattern is formed with up to ten dB differences from what would be expected with no mixed layer—but the interference causes differences smaller than five dB for the three deepest receivers shown in Figure 4. These features are broadly consistent with the observed intensity variations.

Independent predictions of log-amplitude variance were made using Munk-Zachariasen theory to compare to measurements on acoustical signals transmitted during the **PhilSea09** pilot study/ engineering test. This comparison involves 284 Hz center frequency signals transmitted over a 107 km path. Statistics were compared for three paths, one with a single upper turning point at about 60 km,

and two with two upper turning points about 200 km. The theoretical calculation required an estimate of the Fresnel tube structure around the "unperturbed" eigenray. The estimate was made using Bellhop: an example is shown in Figure 6. Predictions for the two paths with deeper upper turning points compare well: predictions for the other path, which has a shallow upper turning point, do not. Estimates of the scintillation index based on log-amplitude are shown in Figure 7. Compare with Figure 3 arrivals 1,2, and 3, respectively.

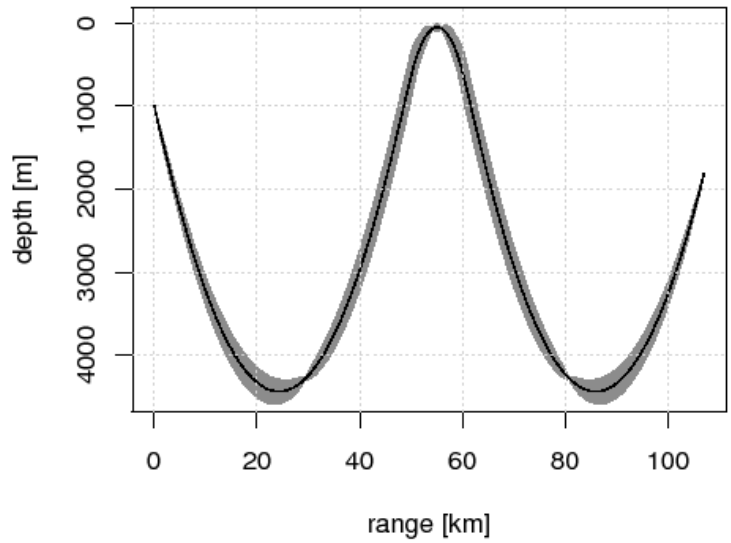


***Figure 6. Fresnel tube around one of the Philippine Sea 2009 experiment eigenrays, frequency 284 Hz.***

These results were presented at the May 2012 Hong Kong Acoustical Society of America meeting for the Asian Marginal Seas special session [8]. A manuscript describing these results has been prepared for the JASA special issue on the Philippine Sea experiment.

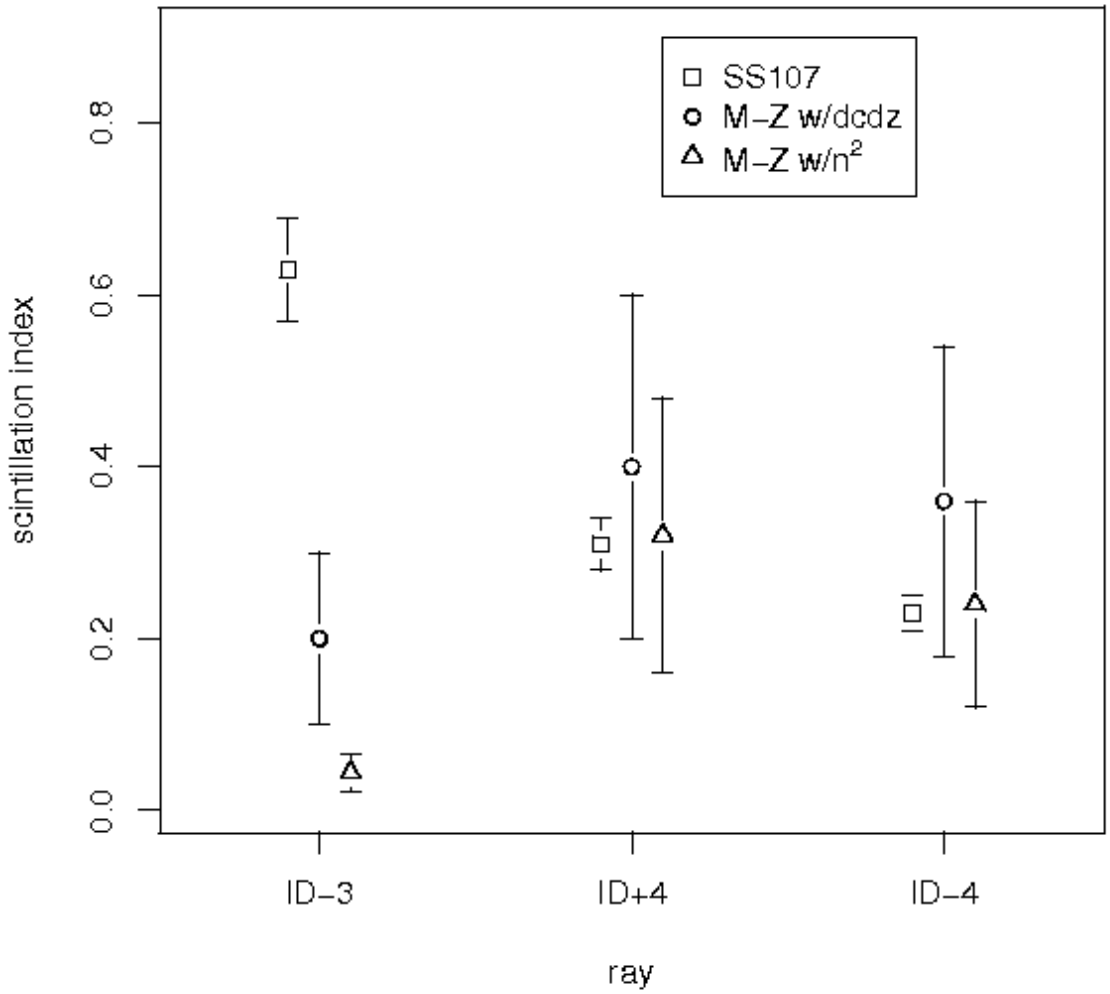


***Figure 7. Measurements and predictions of scintillation index versus path, Philippine Sea 2009 experiment. Two different scales in the theoretical expression were used, one involving the sound speed gradient ("dcdz") and the other using the Brunt-Vaisala frequency ("n^2"). Munk-Zachariasen theory appears to make consistent predictions for paths ("rays") ID+4 and ID-4 at this range and this frequency, but not for path ID-3.***

New results for horizontal statistics of ocean spice and internal waves have been obtained from the Towed CTD Chain (TCTD). Spatial statistics of internal waves and ocean "spice" (neutrally-buoyant thermohaline variations) are important for modeling the effects of oceanic variability on ocean acoustic propagation, to understand and predict phenomena such as acoustic intensity variations and deep fades at receivers. Vertical statistics have traditionally been the focus of pertinent experiments, but little or nothing has yet been learned about the aspect ratio and joint vertical and horizontal statistics in actual measurements, largely due to the difficulty in taking the data required for such analyses. To this end,

APL-UW deployed an 800m version of a towed CTD chain (TCTD) [9] in the **PhilSea10** experiment, attempting to densely sample temperatures and conductivities in a 2D ocean slice along towpaths of order 100km. (See Figure 8 for a notional diagram of the system and the experiment geometry with respect to the rest of that experiment.) While the instrument performed poorly and produced only a small subset of the data expected in the tows, analysis was still possible by taking advantage of a sequence of CTD casts taken nearby in space and time to the analyzed TCTD tow. From analysis of this comparatively small amount of tow data we have obtained horizontal spectra of internal waves and spice, as well as cross-spectra which describe the correlations between multiple sensors in concurrent horizontal towpaths. The latter in particular is new in the literature as far as we are aware – although the original equipment was meant to result in full 2D (horizontal/vertical) spectra, and the heavily troubled tow data prevented calculating this quantity, we can still calculate the cross-spectra between a set of towpaths at different depths. These help constrain the full 2D spectrum as the community develops future models of spice distribution based on field measurements.

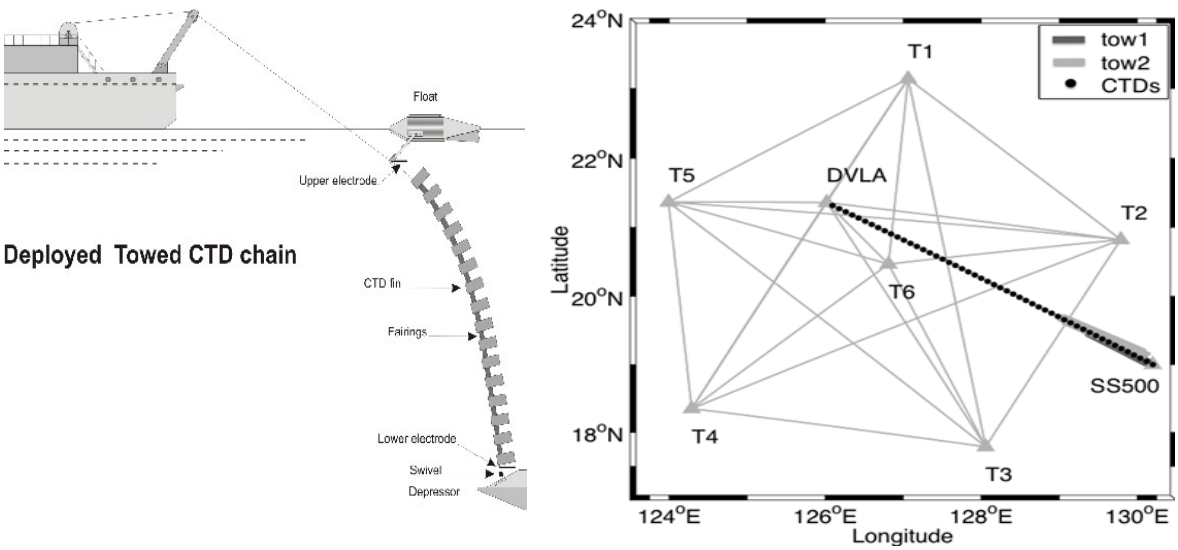


(a) (b)

***Figure 8. (a) Diagram of the 800m towed CTD chain apparatus as deployed behind the ship. (b) The 2010 experiment geometry – a 500km linear sequence of CTDs were taken between the DVLA and ship stop SS500; the two TCTD towpaths overlapped each other and the easternmost 100km of the CTD casts.***

The TCTD pressure, temperature, and salinity measurements are used to compute the density-based and soundspeed-based components of vertical displacement, each via the same equation of state [10], according to the methods of Henyey et al [11]. Other APL-UW work has already focused on studying the vertical variation of spice in the Philippine Sea by similar methods [11,12]. Outside of APL-UW, analysis by Colosi et al [13] takes a different approach to studying that vertical variation. Our horizontal analysis also builds off earlier related works including that by Ferrari and Rudnick [14] and

Klymak and Moum [15]. Those works used undulating towfishes to take CTD measurements at one depth at a time, allowing us to analyze horizontal spectra of internal waves [14,15] and spice [14] in isolation at the one depth. By using a towed chain, we simultaneously measure multiple depths of the same quantities, allowing us to calculate new cross-spectral information. As in Klymak and Moum [15] we present our spectral results in terms of spectra of horizontal gradients in vertical displacement, i.e. "displacement slope".

The analysis relies on linearization of the density and soundspeed measurements around smooth background fields. The great vertical decimation in the TCTD measurements due to equipment malfunctions prevented estimation of these background fields, but by shear serendipity a sequence of CTD casts every 10 km had just been completed along the same path as the tow, and these were used to provide the background field for the analysis. Figure 9 shows the spatial and temporal coverage of the CTD and TCTD data used for the analysis. Tow 1 was not used for the analysis – it had far less coverage of acceptable-quality data, and also did not have the two additional Microcat CTDs attached to the sea cable to assist with the system's troubled pressure measurements (as tow 2 had).

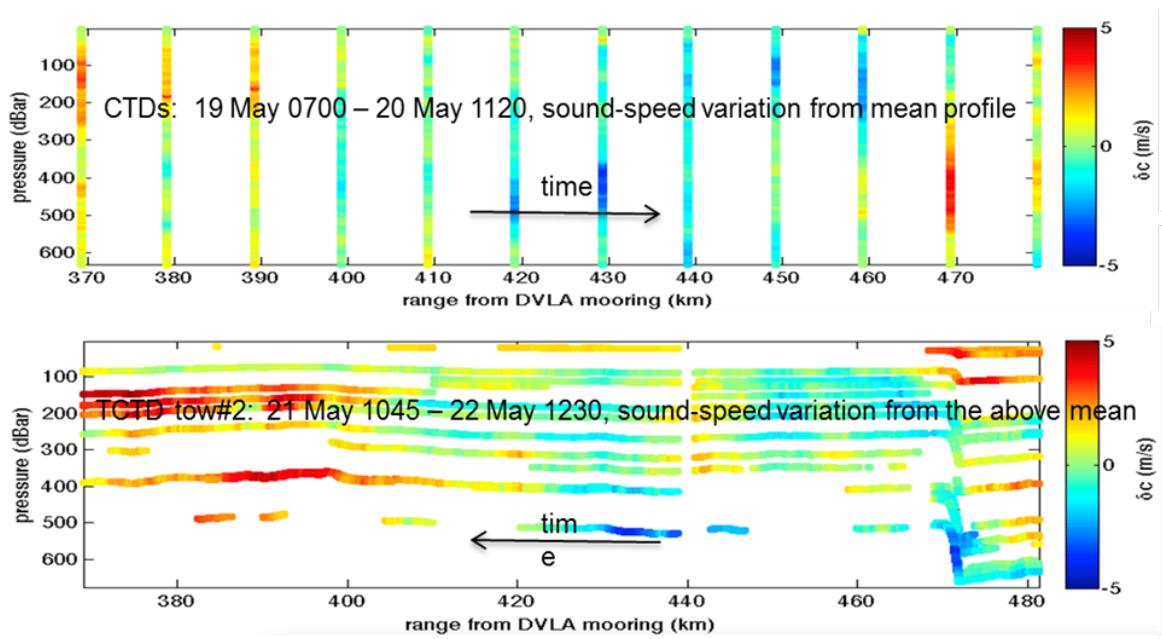


***Figure 9. The data coverage of the CTD data (top) and collocated tow 2 TCTD data (bottom), expressed in plots showing soundspeed variations about the mean of the CTD casts over the TCTD ranges. The CTD casts were taken while sailing away from the DVLA, then at SS500 the ship turned around and started towing the TCTD toward the DVLA.***

The data needed to be extensively cleaned and conditioned. This included: removing outliers and systematically troubled temperature and conductivity data, recalibrating conductivity data by again taking advantage of collocated CTD casts along the tow, fitting a cable model to the particularly poor pressure sensor data with the aid of the Microcat CTDs on the cable, and interpolating the data to

horizontal paths to remove fluctuations due to the pressure changes. However, validation of the spectral results against theoretically predicted patterns, as well as comparisons of aspects of the results with similar results in previously published work, give confidence in the soundness of these results calculated from the **PhilSea10** TCTD.

Figure 10 shows log-log horizontal wavenumber spectra of (Figure 10a) the displacement slopes representing internal wave distribution and in Figure 10b the difference between the soundspeed-based and density-based displacement slopes, representing spice distribution. In Figure 10a the red line is the soundspeed-based displacement slope spectrum, the black line is the density-based displacement slope spectrum, and the green line is the real part of the cross-spectrum between the density- and soundspeed-based displacement slopes. That real part of the spectrum is close to that of the density-based one, and the imaginary part of that same cross-spectrum is not on this plot as it is close to zero, both of which are as theoretically expected. These are theoretically expected given no correlation between the internal waves (which propagate according to wave theory) and spice (which advects); in that case the cross-spectrum should equal the real-valued density-based one, so that there is no real part. Additionally, since the density-based spectrum is due to the internal waves while the soundspeed-based spectrum is due to both internal waves and spice, the soundspeed-based spectrum is higher than the density-based one, as seen in the figure. These density- and soundspeed-based spectra are both variations of the displacement slope spectrum predicted by Garrett Munk (GM) theory [16] – the power level is that of the towed spectrum, while the cut-off wavenumber is the 1e-1 cpm from GM theory multiplied by the ratio of inertial to buoyancy frequencies ($f/N$), and the roll-off continues as $k^{-1}$ from there. At wavenumbers above about 1e-2 cpm, the spectra rise again due to turbulence, as analyzed for example again in Klymak and Moum's papers [15,17]. In Figure 10b the spectra depict spice variability by quantifying the variations in difference between soundspeed-based displacement slope and density-based displacement slope. As in Ferrari and Rudnick's [14] experiment the spice spectra are relatively flat and constant in depth at the depths shown here. The rise in power at high wavenumbers due to turbulence is still seen in the same wavenumber range as in Figure 10a.

Ironically, overall the amount of spice measured on the TCTD chain in the Philippine Sea 2010 experiment was fairly low when analyzed spectrally, which was initially of concern because it conflicted dramatically with the vertical analysis from the CTDs [11]. The spatial representation of the spice in Figure 11 explains the disparity and the irony. As is done in the horizontal analysis, the profiles of spice in Figure 11 are the difference between the soundspeed-based and density-based displacement (the spectra are later calculated from the vertical gradients of these profiles in the vertical analysis). These profiles show a poorly understood minimum in the spice distribution right at the depth range of the TCTD measurements! With a better understanding and ability to model the spice, future experiments may be able to better predict such patterns in the spice in order to measure it more efficiently and consistently.

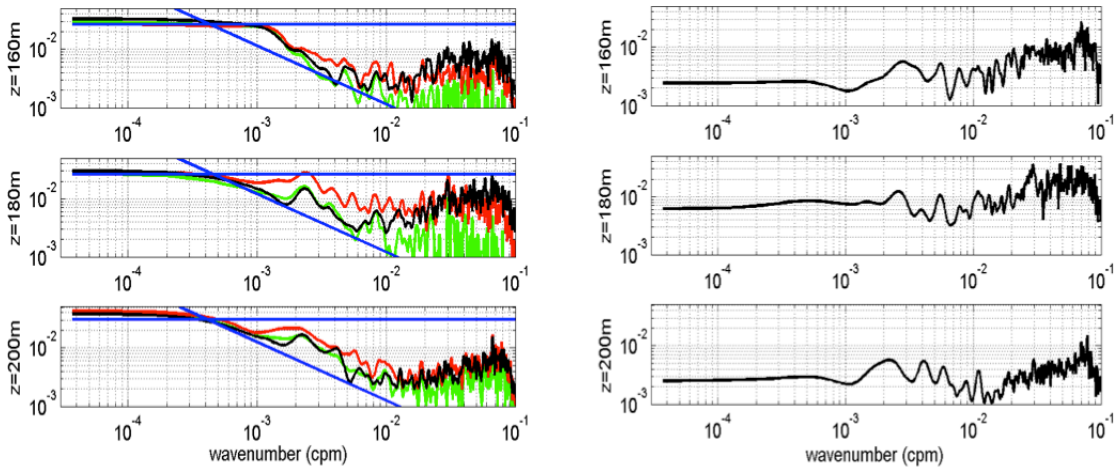


***Figure 10. Log-log horizontal wavenumber spectra of (a) the displacement slope representing internal wave distribution and (b) the difference between the soundspeed-based and density-based displacement slopes, representing spice distribution. Features in these plots are discussed in the text.***

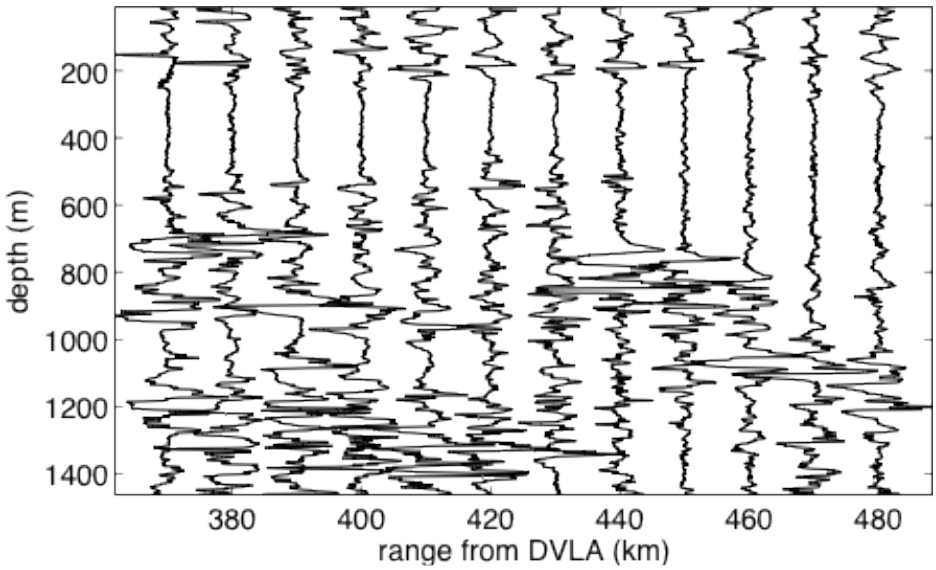


***Figure 11. Spice distribution along the TCTD towpath as calculated from the 12 CTD casts used for the background field. These profiles here are the difference between the soundspeed-based and density-based displacement. Note the ironic (and not well understood) minimum in spice distribution right at the depth span of the TCTD instrument – this can be considered another aspect of the motivation to better understand and model spice, such that new experiments to measure it can do so more efficiently and consistently!***

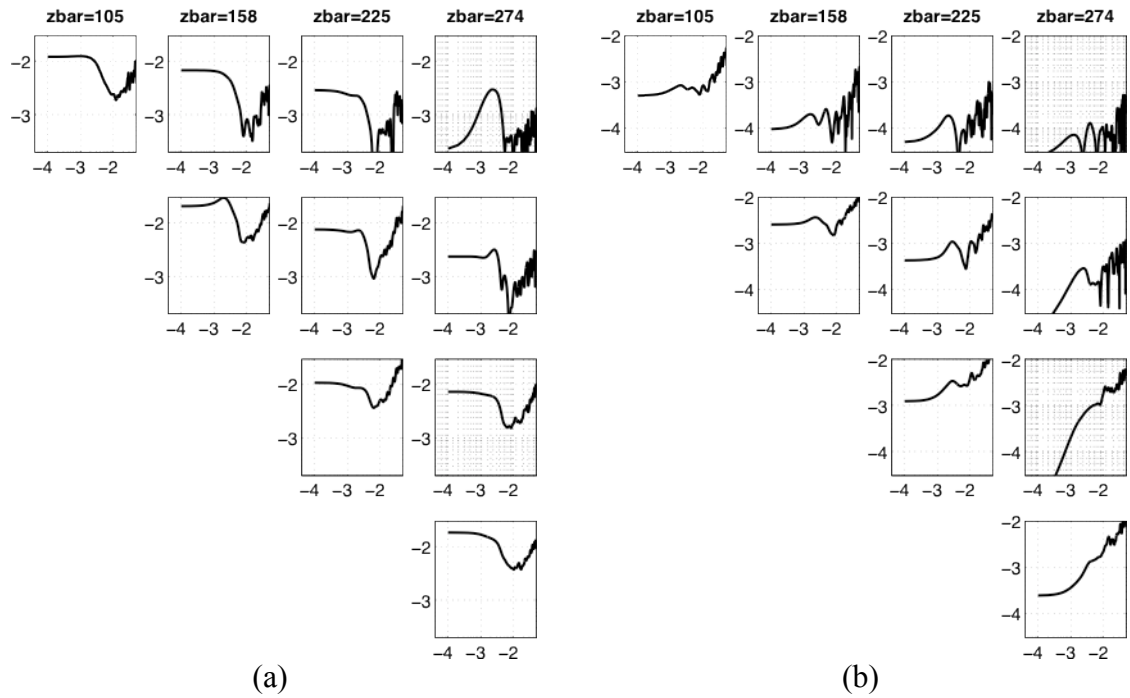


***Figure 12. Arrays of horizontal wavenumber auto- and cross-spectra at four sensor depths, in the mean over the ranges of the tow. The spectra describe the variability in (a) density-based displacement slope representing internal wave distribution, and (b) the difference between the soundspeed-based and density-based displacement slopes representing spice distribution. The arrays in (a) and (b) each depict horizontal cross-spectral combinations at four sensor depths in the towed CTD chain, whose mean depths are list as "zbar" along the tops of the array columns (the arrays of spectra are symmetric so only the upper triangular half of the arrays are shown). The axis labels are minimal to accommodate the many plots: note axes are log-log, x-axes are horizontal wavenumber in cpm, y-axes are power spectral density in meters, and both axes display the log10 of their respective quantity. Features in these plots are discussed in the text.***

The ultimate contribution of the work is a set of auto- and cross-spectra of spice distribution in the horizontal, at a number of simultaneous depths, which may help to constrain the 2D (in x and z) distribution of spice in the ocean. (Or perhaps just in the Philippine Sea at that time of year – it is not yet known if the distribution of spice will be seen as consistently geographically and temporally as the internal wave background seems to be.) Figure 12 shows arrays of horizontal wavenumber auto- and cross-spectra at four sensor depths, in the mean over the ranges of the tow. These spectra describe the variability in Figure 10a the density-based displacement slope representing internal wave distribution, and in Fiugure 10b the difference between the soundspeed-based and density-based displacement slopes representing the spice distribution. The mean depths of each sensor (corresponding to the columns and rows of the array) are list as "zbar" along the tops of the array columns; the arrays of spectra are symmetric so only the upper triangular half of the arrays are shown. In Figure 12a we note internal wave power rolling off at wavenumber similar to that expected by GM theory as in Figure 10a, the power rising again at wavenumbers greater than 1e-2 cpm due to turbulence, and the additional roll-off in the cross-spectra with increasing depth separation of the sensors. Similarly in (12b) we see the rise in power above 1e-2 cpm due to turbulence, roll-off in the spice cross-spectra with increasing

sensor depth separation which is greater than that seen for the internal waves in (10a). Lastly in comparison with Figure 10b we can see a hint in the spectra of at that drop in spice level below about 250m.

The vertical and the horizontal analyses of the CTD and TCTD data are being written up in separate journal papers which are expected to be submitted to JASA in time for the special issue on Deep Water Ocean Acoustics [18].

New results from the LOAPEX data have been obtained using the full resolution of the data. It was found that the first four (southeastern) CTD stations included spice fronts. Figure 13 shows the front at the station 50 km from the receiver array. These fronts invalidate the processing algorithm, because the "background" sound speed profile is assumed to be the low-pass of the sound speed. The sharp fronts are, however, obviously part of the background. These fronts likely have an important effect on acoustic propagation, but without knowing the slope of the front, it is not possible to calculate the effect. Completion of the full resolution reanalysis of the PhilSea data is imminent. We are planning to complete a paper on this subject for the special issue of JASA.

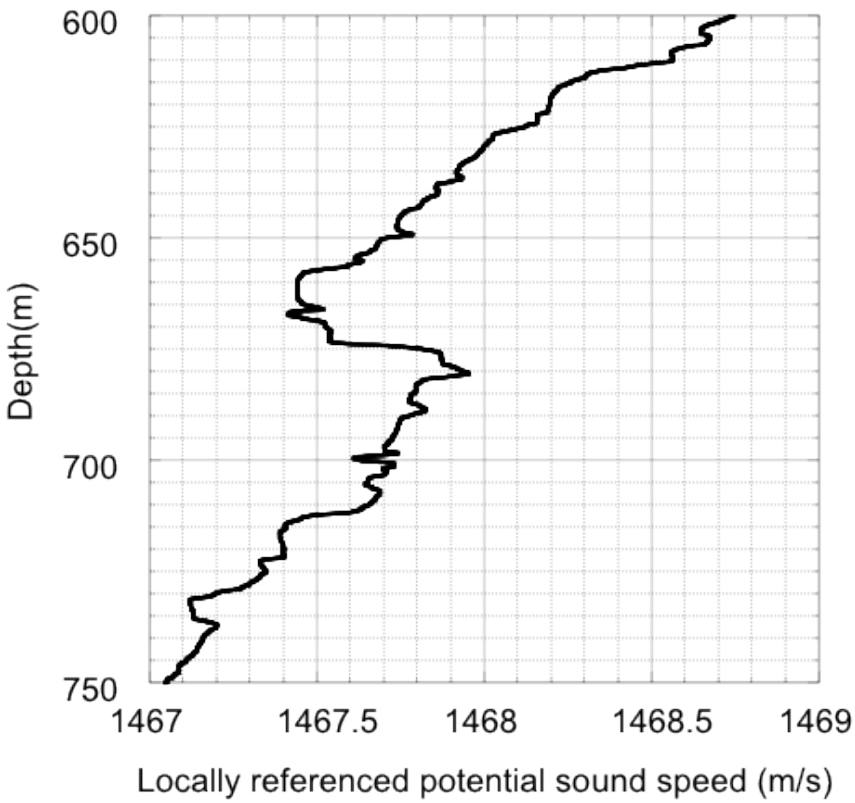


***Figure 13. A spice front at station T50. With such a front, the "background" profile cannot be assumed to contain only low wavenumber content. (The horizontal axis is the sound speed minus the integral from the surface of its adiabatic derivative.) Similar fronts exist at the first four stations, but not beyond.***

Similarly, deducing the vertical properties of the spice from the CTD profiles is insufficient for including them in acoustic propagation without simultaneously understanding their horizontal structure. A beginning on understanding the simultaneous vertical and horizontal structure of spice is an important focus of the work stemming from the data collected with the Towed CTD Chain.

## RELATED PROJECTS AND COLLABORATIONS

A large number of additional investigators have been involved in ONR-supported research related to the NPAL project and participate in the NPAL Workshops, including Art Baggeroer (MIT), J. Beron-Vera (UMiami), M. Brown (UMiami), T. Chandrayadula (NPS), J. Colosi (NPS), N. Grigorieva (St. Petersburg State Marine Technical University), F. Henyey (APL-UW), V. Ostashev (NOAA/ETL), R. Stephen (WHOI), I. Udovydchenkow (WHOI), A. Voronovich (NOAA/ETL), K. Wage (George Mason Univ.), Peter Worcester (Scripps), and others. In addition, we have begun close collaboration with Gerald D'Spain who is funded by the signal processing code of ONR.

Steven R. Ramp, President and CEO, Soliton Ocean Services, Inc., requested APL's PhilSea10 CTD raw data files. These files have been sent and receipt has been acknowledged.

APL-UW provided technical advice to the NOAA Soundscape Mapping Working Group, and at the request of the working group, ambient noise data were sent to the HLS Research, La Jolla, California.

*2006 RSMAS Acoustical Communication Experiment:* We located and collected multiple datasets acquired during a 2006 RSMAS experiment requested by Prof. Brown/ RSMAS/UMiami that used the Kauai ATOC/NPAL source at the end of permitted operations. This experiment transmitted a special signal of Prof. Brown's design. The transmission was captured by multiple APL network receivers. The data collected by the Barber's Point system was deemed to be the best dataset. Due to classification concerns, the raw Barber's Point files were not given to Prof. Brown: instead, single channel acoustical records were stripped out from the raw files. Also located were acoustical records collected by the APL acoustic Seaglider which was deployed in the region for LOAPEX and this experiment. The transmission files from the Kauai computer were recovered and returned to APL. The entire dataset of all pertinent releasable files (Kauai, Barber's Point, and Seaglider) was about 20GB. Everything we could determine about the experiment was documented in an associated memo, and everything shipped to Prof. Brown.

APL-UW supported H.C. Song/MPL with analysis of data collected by the Barber's Point system in order to determine if any of the standard collections captured the acoustic communication signals transmitted during the 2010 LRAC experiment. Transmission loss calculations and power spectral density measurements suggest that the signal at the receiver was too weak to provide useful data.

## IMPACT/APPLICATIONS

This research has the potential to affect the design of long-range acoustic systems, whether for acoustic surveillance, communication, or remote sensing of the ocean interior. The data from the NPAL network, and the special NPAL experiments, indicate that existing systems do not exploit the limits of acoustic coherence at long ranges in the ocean. Estimates of basin-wide sound speed (temperature) fields obtained by the combination of acoustic, altimetry, and other data types with ocean general circulation models have the potential to improve our ability to make the acoustic predictions needed

for matched field and other sophisticated signal processing techniques and to improve our understanding of ocean variability.

**PUBLICATIONS (Refereed)**


Udovydchenkov, Ilya A., Michael G. Brown, Timothy F. Duda, James A. Mercer, Rex K. Andrew, Peter F. Worcester, Matthew A. Dzieciuch, Bruce M. Howe, and John A. Cososi, "Modal analysis of the range evolution of broadband wavefields in the North Pacific Ocean: low mode numbers," *J. Acoust. Soc. Am.,* **131**(6), June 2012.

Udovydchenkov, Ilya A., Ralph Stephen, Timothy Duda, S. Bolmer, Peter Worcester, Rex Andrew, and Bruce Howe, "Bottom interacting sound at 50 km range in a deep ocean environment," *J. Acoust. Soc. Am.,* in press.

Udovydchenkov, Ilya A., Ralph A. Stephen, Timothy F. Duda, S. Thompson Bolmer, Peter F. Worcester, Matthew A. Dzieziuch, James A. Mercer, Rex K. Andrew, and Bruce M, Howe, "Bottom reflections from rough topography in the Long-range Ocean Acoustic Propagation Experiment," *J. Acoust. Soc. Am.,* submitted.

Chandrayadula, Tarun K., Kathleen E. Wage, Peter F. Worcester, Matthew A. Dzieciuch, James A. Mercer, Rex K. Andrew, and Bruce M. Howe, "Reduced rank models for travel time estimation of low mode signals," *J. Acoust. Soc. Am.,* submitted.

Udovydchenkov, Ilya A., Michael G. Brown, Timothy F. Duda, Peter Worcester, Matthew A. Dzieciuch, James A. Mercer, Rex K. Andrew, Bruce M. Howe, and John A. Colosi, "Weekly dispersive modal pulse propagation in the North Pacific Ocean," *J. Acoust. Soc. Am.,* NPAL special issue.

Chandrayadula, Tarun K., Peter F. Worcester, Matthew A. Dzieciuch, James A. Mercer, Rex K. Andrew, and Bruce M. Howe, "Observations and transport theory analysis of low frequency, long range acoustic mode propagation in the Eastern North Pacific Ocean," *J. Acoust. Soc. Am.,* NPAL special issue.

Ganse, A. A., F.S. Henyey, and J.A. Mercer " Horizontal statistics of ocean spice and internal waves measured with a towed instrument chain in the Philippine Sea 2010 experiment," *J. Acoust. Soc. Am.,* NPAL special issue.

Henyey F.S., Jim Mercer, Rex Andrew, and Andrew White, “Smaller-scale internal waves and spice fluctuations on acoustic transmission paths from CTD profiles,” *J. Acoust. Soc. Am.,* NPAL special issue.

Andrew, Rex K., Andrew White, and James A. Mercer, "A test of blue water Rytov theory at 284 Hz and 107 km in the Phillipine Sea," *J. Acoust. Soc. Am.,* NPAL special issue.

Lynch, Stephen D., Gerald L. D'Spain, Kevin D. Heaney, Richard Campbell, Arthur B. Baggeroer, James Mercer, and Peter Worcester, "Dependence of the structure of the shallow first convergence zone in the deep ocean on bathymetry and sound speed variability," *J. Acoust. Soc. Am.*, NPAL special issue.

## REFERENCES


[1] Andrew, Rex K., James A. Mercer, Bradley M. Bell, Andrew A. Ganse, Linda Buck, Timothy Wen, and Timothy M. McGinnis. PhilSea10 APL-UW Cruise Report: 5-29 May 2010, APL-UW TR 1001, October 2010.

[2] Mercer, J. A., Colosi, J. A., Howe, B. M., Dzieciuch, M. A., Stephen, R. A., and Worcester, P. F., "LOAPEX: The Long-range Ocean Acoustic Propagation EXperiment," *IEEE J. Ocean. Eng.,* **34**(1), 1-11, 2009.

[3] RK Andrew, ``APL/UW Removable Hard Drives ", 20 February 2012.

[4] John A. Colosi and Michael G. Brown, "Efficient numerical simulation of stochastic internal-wave-induced sound-speed perturbation fields", J. Acoust. Soc. Am. 103, (4), 1998

[5] S. M. Flatte, R. Dashen, W. H. Munk, K. Watson and F. Zachariasen, *Sound Transmission through a Fluctuating Ocean*, Cambridge University Press, London, 1979.

[6] J. Xu, "Effects of internal waves on low frequency, long range, acoustic propagation in the deep ocean", Doctoral Thesis/Dissertation, Massachusetts Institute of Technology (2007)

[7] L. J. van Uffelen, "Acoustic shadow-zone arrivals at long range in the North Pacific Ocean", Doctoral Thesis/Dissertation, Scripps Institution of Oceanography (2009)

[8] RK. Andrew, AW White, JA Mercer, PF Worcester, MA Dzieciuch, and JA Colosi, ``Theoretical fluctuation predictions for low-frequency acoustical propagation ranges of 25 to 107 km in the 2009-2010 Philippine Sea experiment", Acoustics 2012, Hong Kong, May 2012.

[9] Sellschopp, J., "A towed CTD chain for two-dimensional high resolution hydrography," Deep Sea Research Part I: Oceanographic Research Papers, vol. 44, no. 1, pp. 147-165, Jan. 1997.

[10] Feistel, R. and Hagen, E., "On the GIBBS thermodynamic potential of seawater," Progress In Oceanography, vol. 36, no. 4, pp. 249-327, 1995.

[11] Henyey, F.S., Andrew, R.K., Mercer, J.A., "Small scale internal waves and spice in PhilSea10", 13th NPAL Workshop, 2010.

[12] White A.W., Henyey, F.S., Andrew, R.K., Mercer, J.A., Worcester, P.F., & Dzieciuch, M.A. "Preliminary analysis of PhilSea09 CTD and XBT data", 12th NPAL Workshop, 2009.

[13] Colosi, J. A. et al., "Observations of sound-speed fluctuations in the Western Philippine Sea in the spring of 2009," *in preparation*, 2012.

[14] Ferrari, R. & Rudnick, D. L. L., "Thermohaline variability in the upper ocean," J. Geophys. Res. 105, 16857–16–883, 2000.

[15] Klymak, J. M. & Moum, J. N., "Oceanic Isopycnal Slope Spectra. Part I: Internal Waves," J. Phys. Oc. 37, 1215–1231, 2007.

[16] Munk, W.H., "Internal waves and small-scale processes.," in Evolution of Physical Oceanography: Scientific Surveys in Honor of Henry Stommel, B. A. Warren and C. Wunsch, Eds. Cambridge, MA: MIT Press, 1981, pp. 264-291.

[17] Klymak, J. M. & Moum, J. N., "Oceanic Isopycnal Slope Spectra. Part II: Turbulence," J. Phys. Oc. 37, 1232–1245, 2007.

[18] Ganse A.A. et al., “Horizontal statistics of ocean spice and internal waves measured with a towed instrument chain in the Philippine Sea 2010 experiment,” in preparation for JASA special issue.
[19] Henyey F.S. et al., “Smaller-scale internal waves and spice fluctuations on acoustic transmission paths from CTD profiles,” in preparation for JASA special issue.